Wiley Online Library
Early View publication on www.wileyonlinelibrary.com
(issue and page numbers not yet assigned;
citable using Digital Object Identifier – **DOI**)

Phys. Status Solidi B, 1–7 (2014) / **DOI** 10.1002/pssb.201451200

physica status solidi b
www.pss-b.com
basic solid state physics

Chemical tuning of band alignments for Cu/HfO_2 interfaces

Rajiv Uttamchandani[1,2], Xu Zhang[1], Sadasivan Shankar[3], and Gang Lu[*,1]

[1] Department of Physics and Astronomy, California State University Northridge, Northridge, California 91330, USA
[2] Department of Liberal Arts And Sciences, New York Film Academy, Burbank, California 91502, USA
[3] Technology and Manufacturing Group, Intel Corporation, Santa Clara, California 95054, USA

Received 17 April 2014, revised 19 August 2014, accepted 25 August 2014
Published online 17 September 2014

Keywords computational physics, density functional theory, dielectric/metal gate, work function

[*] Corresponding author: e-mail ganglu@csun.edu, Phone: +1 818 6772021, Fax: +1 818 6773234

First-principles density functional theory is used to explore the possibility of tuning effective work function of high dielectric/metal gate stacks. Using HfO_2/Cu as an example, we demonstrate that the effective work function of the stack can be tuned in a range of ~3.2 eV by incorporating a metallic monolayer at the interface. The calculations reveal that the interfacial charge transfer from the metallic monolayer to the oxide plays a key role in tuning the effective work function. The interfacial charge transfer not only depends on the ionic bonding between the O atoms and the metal monolayer, but it can also be affected by the metallic bonding between the gate Cu atoms and the metal monolayer. The weaker the metallic bonding, the stronger the interfacial dipole moment, and the greater the effective work function modulation. A linear correlation between the interfacial charge transfer and the valence band offset is observed which can be rationalized by an analogy to a parallel plate capacitor. We also find a correlation between interfacial atomic rearrangements and the interfacial charge transfer. The general chemical tuning trends established in this study could potentially provide a valuable guide for designing novel gate materials in conjunction with high-k dielectrics.

1 Introduction The complementary metal oxide semiconductor (CMOS) field effect transistor (FET) made from silicon is the most important electronic device. Over the past 40 years, the number of transistors per integrated circuit chip has continued to double in each technology generation and the minimum feature size in a transistor decreases exponentially each year, following the Moore's law. However, the Moore's law cannot go on forever. It was often said that the lithography and the need for very short wavelengths of light to pattern the minimum feature size limited the Moore's law. But it turns out that materials are key constraints. For instance, the need to maintain high current densities in interconnects recently led to Cu replacing Al as the conductor. The most serious problem, however, is the FET gate stack – the gate electrode (poly-silicon) and the dielectric layer (SiO_2) between the gate and the Si channel. To avoid leakage current, increase transistor-switching speeds, and reduce power consumption, SiO_2 has to be replaced by a high-permittivity (high-k) dielectric and simultaneously the poly-Si to be replaced by a metal gate. It has now been recognized that [1, 2] HfO_2 emerges as a leading candidate to replace SiO_2 gate dielectric thanks to its high permittivity compared to SiO_2, and its ability to be reasonably stable in contact with Si. It has further been realized that the high-k dielectrics must be implemented in conjunction with metal gate electrodes to be effective. However the search for suitable metallic gate materials that optimize compatible work functions, thermal/chemical interface stability and process compatibility with the underlying dielectric has been challenging. In particular, the integration of a metal gate with a high-k dielectric such as HfO_2 requires the effective work function of the metal be within ±0.1 eV of Si-valence and conduction band edges for p- and n-channel MOSFET's, respectively [3–7]. It is well known that the effective work function of a metal gate depends on the underlying dielectric and could differ appreciably from the metal work function in vacuum [8–13]. Therefore to identify the appropriate metal gate material, understanding the factors that control the effective work function at the atomic scale is essential.

In this paper, we investigate the atomic and electronic structure of Cu/HfO_2 interface, with specific interest on how interfacial structure, charge transfer, and chemical bonding

may influence the effective work function of the stack. We choose Cu as the metal gate material because of its application as interconnects in the present CMOS technology. The focus of the paper is to demonstrate the theoretical possibility to tune the effective work function of Cu/HfO_2 stack by introducing a metal monolayer between Cu and HfO_2, inspired by the work of Dong et al. [4]. Thirty different stacks are explored to examine general trends in the effective work function, interfacial charge transfer, and atomic rearrangements.

2 Model and computation

2.1 Computational model Although the most stable phase of HfO_2 in the manufacturing condition is monoclinic (m-HfO_2) [6], we consider here the cubic phase of HfO_2 (c-HfO_2) in the calculations. The justification of this choice is several folds. Firstly, as shown experimentally [14], c-HfO_2 can be created and stabilized in conditions appropriate to CMOS FET devices. Secondly, c-HfO_2 thus created can have a dielectric constant $k \sim 50$, much higher than the corresponding value ($k \sim 17$) in m-HfO_2. Thirdly, c-HfO_2 has clean and well-defined surfaces and most importantly, its lattice constant matches well with that of Cu, significantly reducing the possible interfacial strain. Lastly, the computational cost of modeling c-HfO_2 is much cheaper than that of modeling m-HfO_2, which allows us to examine many more materials than otherwise possible.

We use a double-interface model without a vacuum gap, shown in Fig. 1, as the supercell of the first-principles modeling of the Cu/m/HfO_2 stacks (here "m" denotes a metal monolayer). Hence, the artificial electric field associated with the vacuum model is eliminated. The supercell has seven Cu (100) layers, along with six underlying HfO_2 (100) layers, which are sufficient to yield converged results [2]. For the sandwiched stacks, a metal monolayer is placed in between the two identical Cu–HfO_2 interfaces.

The equilibrium lattice parameters obtained from the bulk relaxations for c-HfO_2 and fcc-Cu are 5.062 and 3.640 Å, respectively. For the interface, Cu[100] is placed parallel to c-HfO_2[100]. Thus by imposing the lateral lattice constant of the supercell to that of c-HfO_2, we obtain a very small interfacial mismatch of 1.6%. To determine energetically favorable lateral mapping for Cu/HfO_2 and Cu/m/HfO_2 stacks, we calculate the interfacial energy of a stack as

$$E_{\text{int}} = \frac{E_{\text{tot}} - nE_{\text{HfO}_2} - mE_{\text{Cu}} - lE_{\text{m}} - k\mu_{\text{O}}}{2S}, \qquad (1)$$

where E_{tot} is the total energy of the stack. E_{HfO_2}, E_{Cu} and E_{m} is the energy of the bulk HfO_2, Cu and the inserted metal, respectively. n, m, and l represents the number of HfO_2 units, Cu atoms, and the inserted metal atoms, respectively. μ_{O} is the chemical potential of oxygen in O_2 molecule and k indicates the number of excess O atoms in the stacks. S is the interface area. The more negative the interfacial energy, the more stable the interface. The interfacial energy E_{int} corresponding to the lateral mappings in Fig. 2a–f is: −0.02, −0.77, −0.70, −0.24, −1.0, and −1.22 J/m^2, respectively. Therefore, the most stable mapping for the Cu/HfO_2 interface involves a direct placement of Cu atoms on top of O atoms in HfO_2 as shown in Fig. 2f. We have also examined the Hf-rich interface, but found its energy (1.88 J/m^2) much higher than that of the oxygen-rich interface (−1.22 J/m^2). Therefore, in all calculations, c-HfO_2 is terminated with a layer of O instead of Hf as shown in Fig. 1. Our choice of the oxygen-rich interface is also supported by the work of Tse and Robertson [8], in which the O-rich interface was found to be the most stable at a high O chemical potentials. In addition, we have also examined the most stable mapping of Cu–m–HfO_2 in the oxygen-rich interface for different metallic monolayers. We find that the most stable mapping of the stack involves Cu grown epitaxially on top of the monolayer metal atoms, which in turn is placed on the fourfold site, as shown in Fig. 2g.

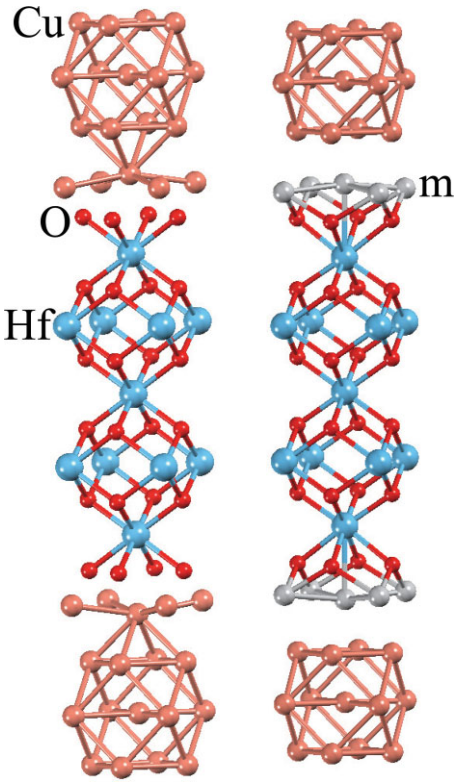

Figure 1 Schematic of the double interface supercell used in our calculations. On the left is the supercell for Cu/HfO_2 interfaces and on the right, two metal monolayers are sandwiched between Cu and HfO_2. The bronze, red, blue and silver spheres represent Cu, O, Hf and the monolayer metal atoms, respectively.

2.2 Computational parameters All calculations were performed using first-principles spin-polarized Density Functional Theory (DFT) as implemented in the Vienna Ab-initio Simulation Package [15, 16], with the Generalized Gradient Approximation (GGA) [17] for the exchange and correlation functional. Ultrasoft pseudopotentials [18] were used and k-point meshes were generated following

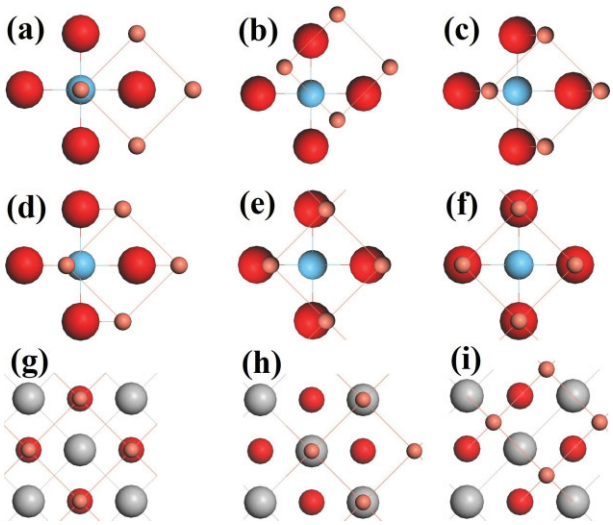

Figure 2 Schematic of various lateral interface mappings explored for the Cu/HfO_2 stack in (a)–(f) and the Cu–m–HfO_2 stacks in (g)–(i). The bronze, red, blue and silver spheres represent Cu, O, Hf, and m atoms, respectively.

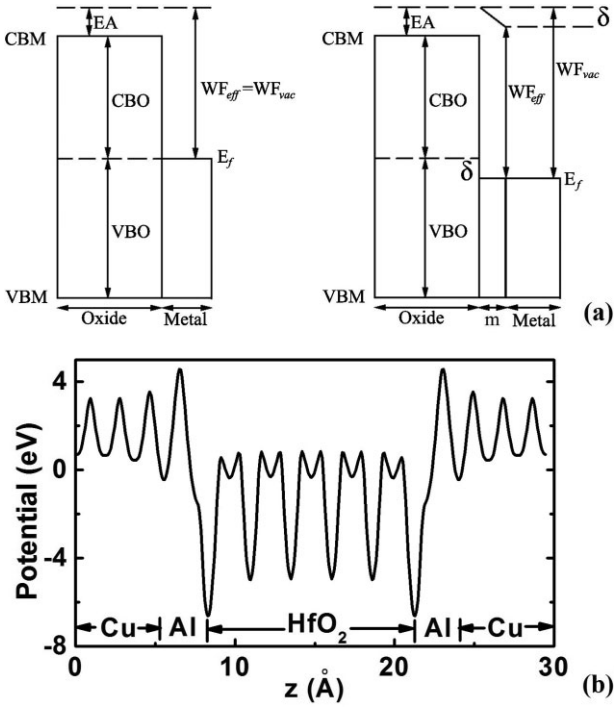

Figure 3 (a) Band diagram for the metal/oxide interface. Left, the interface without charge transfer. Right, with charge transfer from the metal to the oxide. Notations: WF_{vac} for vacuum work function of the metal gate, WF_{eff} for the effective work function of the stack, E_f for the metal Fermi energy, EA for the oxide electron affinity, VBM for the oxide valence band maximum, VBO for the valence band offset between the metal and the oxide, CBM for the oxide conduction band minimum, CBO for the conduction band offset between the metal and the oxide, m for the metal monolayer and δ for the vacuum level discontinuity. (b) Variation of the electrostatic potential along the [001] direction for Cu–Al–HfO_2 stack.

the Monkhorst–Pack scheme [19], centered at the Gamma point. Energy cutoff for plane waves was set to 400 eV, along with a Gaussian smearing of 0.2 eV. For the double-interface calculations, a $10 \times 10 \times 1$ k-point mesh was used. Subsequent density of states (DOS) analysis of these systems was performed with a $16 \times 16 \times 1$ k-point mesh. For calculations involving different Cu/HfO_2 and Cu/m mappings, a $10 \times 10 \times 2$ k-point mesh was used instead. For calculations of the vacuum work function, we also used a $10 \times 10 \times 1$ k-point mesh, with a 15 Å vacuum gap between the terminating surfaces. All systems investigated here were relaxed until the residual forces between atoms were less than 0.01 eV/Å. We also performed volume relaxations of the supercell to eliminate the residual stress.

2.3 Valence band offset (VBO) calculation In Fig. 3, we present schematic band diagrams, which indicate VBO along with other quantities discussed in this paper. We use a method due to Van de Walle and Martin (WM) [20], often called "standard bulk-plus-lineup approach", to calculate the VBO. In the WM approach, the VBO is determined as the difference between the properly shifted metal Fermi energy (defined as the difference between the bulk Fermi level and the bulk planar averaged electrostatic potential), and the properly shifted oxide valence band maximum or VBM (defined as the difference between the VBM of the bulk oxide and its bulk planar averaged electrostatic potential). More specifically,

$$\mathrm{VBO} = \Delta\bar{V}_{\mathrm{int}} + \Delta E_{\mathrm{bulk}}, \tag{2}$$

where $\Delta\bar{V}_{\mathrm{int}} \equiv \bar{V}_{\mathrm{m}} - \bar{V}_{\mathrm{O}}$. $\bar{V}_{\mathrm{m}}$ is the averaged electrostatic potential of Cu/m interface and $\bar{V}_{\mathrm{O}}$ is the averaged electrostatic potential of HfO_2 in the stack. $\Delta E_{\mathrm{bulk}} \equiv (E_{\mathrm{F,m}} - \bar{V}_{\mathrm{m}}) - (E_{\mathrm{VBM,O}} - \bar{V}_{\mathrm{O}})$ is from bulk calculations, where $E_{\mathrm{F,m}}$ and $E_{\mathrm{VBM,O}}$ are the Fermi energy of the metal and VBM of the oxide, respectively. In the WM method, contributions to the VBO come from the electrostatic potentials of both the stack and the bulk, which as seen in Fig. 3b converge very quickly after just one layer away from the interface. Therefore, the WM method of calculating the VBO presents to be fairly accurate within the confines of DFT.

However, it is well known that the conventional DFT calculations of transition metal oxides suffer from an error originated from the lack of derivative discontinuity of the exchange-correlation potential [21]. As a result, the energy levels such as VBM cannot be calculated accurately. In contrast, a many-body Green's function theory known as the GW method has been successfully used to calculate the VBM values of the oxides [22]. We therefore use the GW correction (+0.57 eV from Ref. [6]) for the VBM of c-HfO_2, and apply this correction to the VBO and the effective work function values (see the next section). All the above corrections, however, add nothing more than a constant shift to the effective work function for all systems investigated.

Table 1 The VBO, the effective work function $\Phi_{m,eff}$, the vacuum work function $\Phi_{m,vac}$ of Cu/m composite, the interfacial dipole moment μ_{int}, the rumpling, the overlap parameters, and the interfacial energy E_{int} for 30 different stacks. $\Phi'_{m,eff}$ is the effective work function calculated using the phenomenological model in Ref. [9] based on μ_{int}. χ is the Pauling electronegativity of the metal monolayer. All values except for the rumpling parameters (in Å), the overlap parameters (in arbitrary unit) and the interface energy (J/m^2) are reported in eV.

stack	VBO	$\Phi_{m,eff}$	$\Phi_{m,vac}$	μ_{int}	rumpling	overlap	E_{int}	$\Phi'_{m,eff}$	χ
Cu/Hf/HfO_2	4.00	4.60	4.60	0.33	0.0268	2.74	−4.08	4.54	1.30
Cu/Ta/HfO_2	3.97	4.63	4.63	0.33	0.0258	1.80	−3.13	4.54	1.50
Cu/Ti/HfO_2	3.80	4.80	4.76	0.34	0.0314	1.70	−6.59	4.65	1.54
Cu/Nb/HfO_2	3.78	4.82	4.78	0.35	0.0206	1.85	−3.84	4.76	1.60
Cu/W/HfO_2	3.77	4.83	4.76	0.35	0.0207	2.26	0.18	4.76	2.36
Cu/V/HfO_2	3.72	4.88	4.80	0.34	0.0312	1.97	−4.70	4.65	1.63
Cu/Zr/HfO_2	3.76	4.84	4.80	0.37	0.0197	1.68	−4.57	4.97	1.33
Cu/Mo/HfO_2	3.52	5.08	4.72	0.37	0.0137	2.35	−1.16	4.97	2.16
Cu/Cr/HfO_2	3.37	5.23	4.75	0.39	0.0137	2.40	−3.15	5.18	1.66
Cu/Re/HfO_2	3.29	5.31	4.68	0.40	0.0107	2.71	1.72	5.29	1.90
Cu/Mn/HfO_2	3.18	5.42	4.64	0.43	0.0097	3.95	−3.97	5.61	1.55
Cu/Co/HfO_2	3.17	5.43	4.66	0.42	0.0114	4.97	−1.50	5.50	1.88
Cu/Fe/HfO_2	3.09	5.51	4.67	0.42	0.0123	4.71	−2.96	5.50	1.83
Cu/Tc/HfO_2	3.07	5.53	4.66	0.42	0.0113	2.85	0.06	5.50	1.90
Cu/Al/HfO_2	3.06	5.54	4.71	0.45	0.0017	0.95	−5.51	5.83	1.61
Cu/Os/HfO_2	2.79	5.81	4.70	0.47	−0.0001	2.73	1.31	6.04	2.20
Cu/Ni/HfO_2	2.66	5.94	4.60	0.46	0.0036	4.77	−1.31	5.93	1.91
Cu/Zn/HfO_2	2.61	5.99	4.64	0.47	0.0047	3.72	−2.76	6.04	1.65
Cu/Ru/HfO_2	2.47	5.93	4.66	0.48	−0.0013	2.88	0.99	6.15	2.20
Cu/Rh/HfO_2	2.41	6.19	4.60	0.49	−0.0015	3.78	0.11	6.25	2.28
Cu/Ir/HfO_2	2.36	6.24	4.64	0.51	−0.0008	3.69	1.11	6.46	2.20
Cu/Sc/HfO_2	2.32	6.28	4.96	0.50	−0.0009	1.57	−0.94	6.36	1.36
Cu/Ga/HfO_2	1.94	6.66	4.64	0.52	0.0000	0.91	0.39	6.57	1.81
Cu/Pd/HfO_2	1.83	6.77	4.62	0.55	−0.0040	4.85	0.04	6.89	2.20
Cu/Y/HfO_2	1.57	7.03	4.58	0.56	−0.0037	1.88	0.46	7.00	1.22
Cu/Pt/HfO_2	1.41	7.19	4.74	0.57	−0.0024	4.62	0.18	7.11	2.28
Cu/HfO_2	1.37	7.23	4.57	0.51	0.0052	5.17	−1.22	6.47	1.90
Cu/Au/HfO_2	1.01	7.59	4.66	0.60	−0.0065	5.21	0.34	7.43	2.54
Cu/Ag/HfO_2	0.97	7.63	4.67	0.61	−0.0062	5.33	0.50	7.54	1.93
Cu/Cd/HfO_2	0.73	7.87	4.52	0.64	−0.0073	2.15	−0.18	7.86	1.69

2.4 Effective work function calculation The primary quantity of interest is the effective work function ($\Phi_{m,eff}$) of the stack. This quantity is trivially related to the calculated VBO as

$$\Phi_{m,eff} = BG_O + EA_O - VBO, \quad (3)$$

where BG_O is the oxide band gap and EA_O is the electron affinity of the bulk oxide (see Fig. 3). Because of the well-known failures of DFT/GGA in determining band gaps and electron affinity, we hereby use experimental values of the oxide band gap (5.7 eV from Ref. [23]) and the oxide electron affinity (2.9 eV from Ref. [24]) to determine the effective work function of Cu/m/HfO_2 stack.

3 Results and discussion A total of 30 Cu/m/HfO_2 stacks are studied in this paper. The results reported in this paper are intended to be semi-quantitative, owing to the well-known limitations of DFT/GGA for calculating band offsets. The primary goal of the paper is to examine the general trends and gain physical insight for the stack systems as the metallic monolayer varies across transition metal element series.

The main results of VBO and $\Phi_{m,eff}$ are summarized in Table 1. We observe a wide variation of VBO (∼4.0 eV) and the effective work functions (3.2 eV), affirming the effectiveness of the proposed chemical tuning. Additional surface calculations of Cu and Cu/m interface were performed to obtain the vacuum work functions of pure Cu and Cu/m composites, respectively as displayed in Table 1. It is found that the vacuum work functions of various Cu/m composites vary by a maximum of ∼0.4 eV, in contrast to the variations of the effective work functions of the Cu/m/HfO_2 stacks. Since the vacuum work functions of the Cu/m composites are dominated by the surface properties of Cu, the metallic monolayer does not change considerably the vacuum work function of the Cu gate. Therefore, it is interesting to understand the origin of the large variations of the effective work functions. In the following, we show that the effective work functions correlate to the interfacial dipole moments, which depend sensitively on the interfacial charge transfer

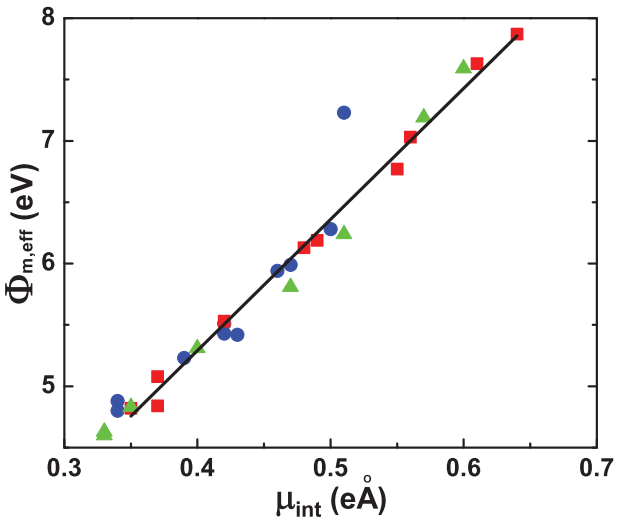

Figure 4 A linear relationship between VBO and the interfacial dipole moment. The circular (blue), square (red), and triangular (green) symbols represent the metal monolayer in the first, second, and third row of the transition metal series in the periodic table, respectively.

due to the incorporation of the metallic monolayer. The significant changes of the interfacial dipole moments lead to the large variations of the effective work functions.

3.1 Charge transfer and interface dipole We find that the primary contribution to the effective work function is interfacial charge transfer. The metallic monolayer can modulate the interfacial charge transfer thus tune the effective work function. Here we use charge transfer induced dipole moment across the metal/oxide interface to quantify the charge transfer. Since we are mainly interested in the charge transfer from the metal monolayer to the oxide, we calculate the interfacial dipole moment perpendicular to the interface (in the z direction) as

$$\mu_{\text{int}} = -e \int_{\text{cell}} z \Delta\rho(x, y, z) \mathrm{d}x\mathrm{d}y\mathrm{d}z, \tag{4}$$

where $\Delta\rho$ is the bonding charge density defined as the difference between the bulk charge density and the superposition of atomic charge densities in the supercell; the integral is performed over an half of the supercell due to the symmetry and the origin is at the center of the supercell. As shown in Table 1, the dipole moments are all positive, indicating that charge transfer occurs from the metal monolayer to the oxide in all cases. More importantly, we find a near linear relationship between the interfacial dipole moments and the VBO values for the 30 stacks as shown in Fig. 4—the greater the charge transfer, the lower the VBO value, and the higher the effective work function. This can be understood from an analog to an infinite parallel plate capacitor, containing charge $+Q/-Q$ on opposing surfaces separated by a distance d. The charge Q corresponds to the charge transfer amount across the interface and d represents the interlayer distance between the metal monolayer and the oxide. The potential drop across this capacitor is thus given by

$$V_{\text{C}} = \frac{Qd}{\varepsilon_0 \varepsilon_{\text{r}} A} = \frac{\mu_{\text{int}}}{\varepsilon_0 \varepsilon_{\text{r}} A}, \tag{5}$$

where A is the interfacial area, ε_0 is the permittivity in vacuum, and ε_{r} is the effective interfacial dielectric constant. The linear relationship is thus obtained between V_{C} and μ_{int}. Since VBO is primarily determined by the potential drop at the interface, the linear relationship should also hold between VBO and the interfacial dipole moment. The potential drop is clearly seen in Fig. 3b from the metal to the oxide, providing driving force for charge transfer. Incidentally, the linear relation implies that different Cu/m/HfO_2 stacks have a similar effective interfacial dielectric constant ε_{r}.

In Table 1, we also calculate the effective work functions ($\Phi'_{\text{m,eff}}$) based on a phenomenological model that directly connects the effective work function with the interfacial dipole moment [9, 10]. These $\Phi'_{\text{m,eff}}$ values are in an excellent agreement with those ($\Phi_{\text{m,eff}}$) determined from our first-principles calculations. This comparison validates the model and establishes a linear relationship between the effective work function and the interfacial dipole moment. The effective work function is also correlated to the electronegativity of the metal monolayer; the greater the electronegativity of the metal, the larger the effective work function. This correlation could be used in the engineering design of heterostructure stacks [25]. Finally, the interfacial energy is related to the electronegativity of the inserted metal as well. As shown in Table 1, in general, the greater the electronegativity of the metal, the more positive the interfacial energy. This can be understood from the fact that the metal monolayer with a greater electronegativity loses less charges to O, thus has a weaker ionic bonding to the O layer, and a higher interfacial energy. Note that some of the interfacial energies are positive under conditions where the chemical potential of O is below -3.5 eV, which would render the interfaces unstable. However, for the most cases of interest [8], the O chemical potential is greater than -3.5 eV, hence the interfaces are stable and the effective work functions computed are reliable.

3.2 Bonding and charge transfer To shed light into the nature of interfacial charge transfer, we calculate the bonding charge density (Fig. 5) and the local density of states (LDOS) of the interfacial atoms (Fig. 6). We find that the interfacial charge transfer is highly localized, occurring primarily from the monolayer metal atoms to the first layer O atoms. The interfacial charge transfer competes with the bulk charge transfer from Hf atoms to the first layer O atoms in the bulk of the oxide. More importantly, a metallic bonding between the gate Cu atoms and the monolayer atoms is developed. This metallic bonding interferes with the interfacial ionic bonding, i.e., the stronger the metallic bonding between Cu–m, the weaker the charge transfer across the interface. For example, as shown in Figs. 5 and 6, the ionic bonding between Au (or Cu) with O across the interface is

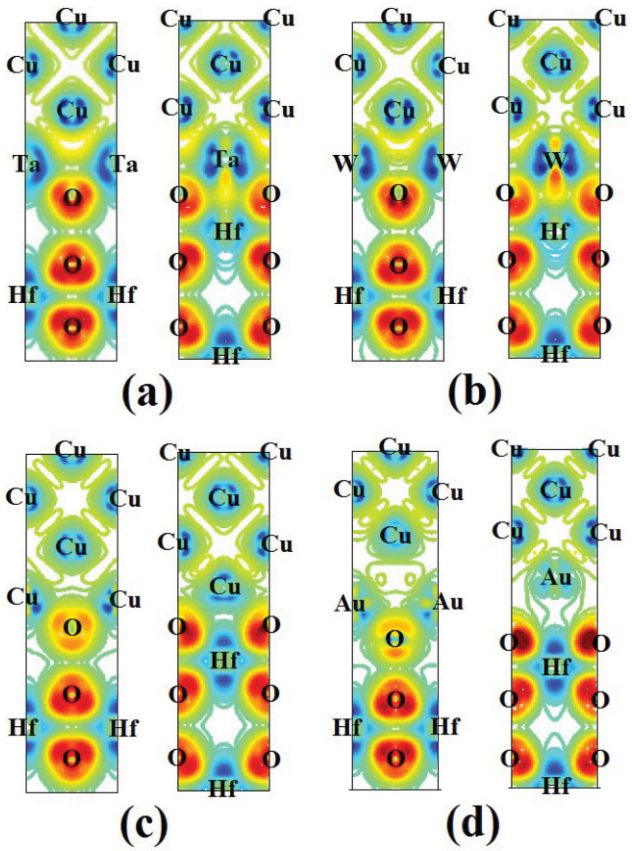

Figure 5 The bonding charge density (in $Å^{-3}$) in plane I (left) and plane II (right) for each stack. The planes I and II are indicated in Fig. 7. The density contour scale ranges from −0.29 (blue) to 0.29 (red). The positive (negative) value represents the accumulation (depletion) of charge density. (a) Cu/Ta/HfO_2, (b) Cu/W/HfO_2, (c) Cu/HfO_2, and (d) Cu/Au/HfO_2.

much stronger than that between Ta (or W) and O. This is because the metallic bonding of Au–Cu and Cu–Cu is much weaker than that of Ta–Cu and W–Cu, as shown in Fig. 5. In case of Cu/HfO_2, the metallic bonds are formed by the hybridization between Cu $3d_{z^2}^2$ and $3d_{yz}$ orbitals and O 2p orbitals. It is through this metallic bonding, the effective work function is modulated. For instance, to increase the effective work function by a larger amount, one should seek a metal monolayer that has very little bonding to the gate metal, thus the interfacial charge transfer is greater, leading to a more pronounced increase of the effective work function. Although our calculations are based on Cu gate, the conclusion should be valid for other metal gate materials as well.

We can quantify the strength of the ionic bonding via the overlap between the monolayer metal states and the O states, defined as the following

$$\text{Overlap} = \int_{-\infty}^{E_F} \text{LDOS}(E;\text{m}) \times \text{LDOS}(E;\text{O})\text{d}E, \qquad (6)$$

where LDOS(E; m) and LDOS(E; O) are the local density of state of the monolayer metal and O atoms, respectively.

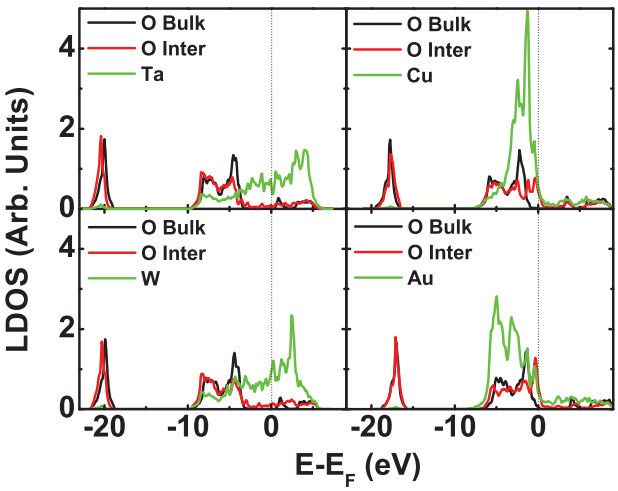

Figure 6 The LDOS (arbitrary units) on the interfacial O atom (red), the bulk O atom (black), and the monolayer metal atom (green) in each Cu/m/HfO_2 stack. The Fermi energy of each stack is denoted by the vertical dashed line.

As shown in Table 1, the overlap values are 5.17 and 5.21 for Cu and Au, respectively, which are much larger than 1.80 and 2.26 for Ta and W, respectively. And the charge transfer amount in Cu/HfO_2 (0.51 eÅ) and Cu/Au/HfO_2 (0.61 eÅ) stacks is greater than that in Cu/Ta/HfO_2 (0.33 eÅ) and Cu/W/HfO_2 (0.35 eÅ).

All stacks shown here are metallic—there is a finite DOS at the Fermi energy, owing to the delocalized states of the monolayer metal atoms. Moreover, the interfacial charge transfer spreads onto O atoms and renders the insulating O layer metallic. This can be observed most clearly in Cu/Au/HfO_2 stack. The overall energy shift in LDOS of bulk O atoms is due to the potential drop at the interface; the greater the potential drop, the larger the energy shift.

3.3 Structural relaxation The interfacial charge transfer usually accompanies atomic rearrangements at the interface. As an indication of local atomic rearrangements at the interface, rumpling parameter [5] $R = (d_O - d_{Hf})$ is evaluated; here d_O represents the distance between O atoms in the first and second layer of the oxide and d_{Hf} is the distance between the Hf atoms at the same layers (as shown in Fig. 7). A larger rumpling parameter indicates a greater atomic rearrangement at the interface. To understand the trend in rumpling parameters, we calculate the dipole moment between the first layer O and Hf atoms, μ_{O-Hf} as displayed in Fig. 7; the O–Hf dipole moment points to the opposite direction with respect to the interfacial dipole μ_{int}. As shown in Fig. 7c, the rumpling parameter increases with an increasing charge transfer between O and Hf atoms for the three series of transition metal elements. This is because a larger Hf–O dipole leads to a larger rumpling parameter. On the other hand, owing to the competition between the interfacial charge transfer and bulk charge transfer in the oxide, a greater interfacial charge transfer results in a smaller Hf–

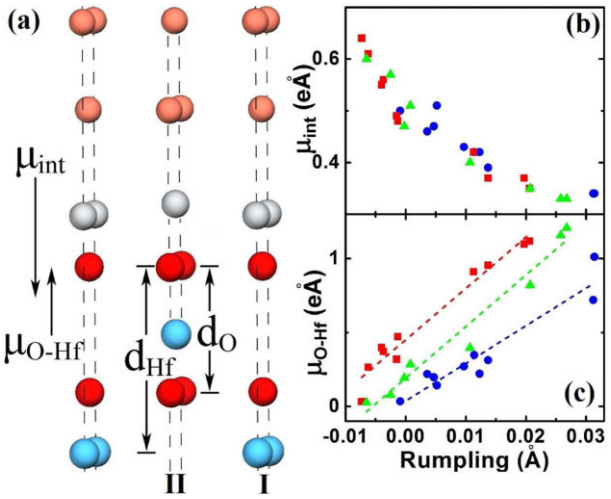

Figure 7 (a) Illustration of the rumpling parameter and the dipole moments. The bronze, red, blue, and silver spheres represent Cu, O, Hf and the monolayer metal atoms, respectively. (b) Correlation between the interfacial dipole moment μ_{int} and the rumpling parameters, and (c) correlation between μ_{O-Hf} and the rumpling parameters. Circular (blue), square (red), and triangular (green) symbols represent the metal monolayer in the first, second and third row of the transition metal series in the periodic table, respectively.

O dipole, thus a smaller rumpling parameter as observed in Fig. 7b.

4 Conclusion We have explored theoretical feasibility of tuning the effective work function of high-*k*/metal gate stacks by incorporating a metallic monolayer at the interface. Using first-principles DFT calculations, we have examined 30 Cu/m/HfO_2 stacks where the monolayer involves different but primarily transition metal elements. A tuning range of $\sim$ 3.2 eV for the effective work function can be achieved for the Cu gate. It is found that the interfacial charge transfer from the metallic monolayer to the oxide plays a key role in tuning the effective work function. The interfacial charge transfer not only depends on the ionic bonding between O and the metal monolayer, but it can also be modulated by the metallic bonding between the gate Cu atoms and the metal monolayer. The weaker the metallic bonding, the stronger the interfacial dipole moment, and the greater the effective work function modulation. A linear correlation between the interfacial charge transfer (or the dipole moment) and the VBO is observed which can be rationalized by an analogy to a parallel plate capacitor. We also find a correlation between the rumpling parameters and the interfacial charge transfer. The general chemical tuning trends established in this study could potentially provide a valuable guide for designing novel gate materials in conjunction with high-*k* dielectrics.

Acknowledgements We thank Yi Zhao for assistance in preparing the figures. The work was supported by Intel Corporation and NSF-PREM grant (DMR-1205734).

References

[1] H. J. Park, Y. M. Sun, H. Troiani, P. Santiago, M. J. Yacaman, and J. M. White, Surf. Sci. **521**, 1–9 (2002).
[2] L. R. C. Fonseca and A. A. Knizhnik, Phys. Rev. B **74**, 195304 (2006).
[3] G. D. Wilk, R. M. Wallace, and J. M. Anthony, Appl. Phys. Rev. **89**, 5243–5275 (2001).
[4] Y. F. Dong, S. J. Wang, Y. P. Feng, and A. C. H. Huan, Phys. Rev. B **73**, 045302 (2006).
[5] M. Nunez and M. B. Nardelli, Phys. Rev. B **73**, 235422 (2006).
[6] X. Luo, A. A. Demkov, D. Triyoso, P. Fejes, R. Gregory, and S. Zollner, Phys. Rev. B **78**, 245314 (2008).
[7] C. Marchiori, M. M. Frank, J. Bruley, V. Narayanan, and J. Fompeyrine, Appl. Phys. Lett. **98**, 052908 (2011).
[8] K. Y. Tse and J. Robertson, Phys. Rev. Lett. **99**, 086805 (2007).
[9] H. Zhu and R. Ramprasad, Phys. Rev. B **83**, 081416(R) (2011).
[10] H. Zhu, C. Tang, L. R. C. Fonseca, and R. Ramprasad, J. Mater. Sci. **47**, 7399–7416 (2012).
[11] A. Kiejna and K. F. Wojciechowski, Metal Surface Electron Physics (Pergamon, Oxford, 1996).
[12] R. Ramprasad, P. von Allmen, and L. R. C. Fonseca, Phys. Rev. B **60**, 6023– 6027 (1999).
[13] B. H. Lee, S. C. Song, R. Choe, and P. Kirsch, IEEE Trans. Electron Devices **55**, 8–20 (2008).
[14] S. Migita, Y. Watanabe, H. Ota, H. Ito, Y. Kamimuta, T. Nabatame, and A. Toriumi, Symp. VLSI Technol., pp. 152–153 (2008).
[15] G. Kresse and J. Hafner, Phys Rev. B **47**, 558–561 (1993).
[16] G. Kresse and J. Furthmuller, Comput. Mater. Sci. **6**, 15 (1996); Phys. Rev. B **54**, 11169–11186 (1996).
[17] J. P. Perdrew, J. A. Chevary, S. H. Vosko, K. A. Jackson, M. R. Pederson, D. J. Singh, and C. Fiolhais, Phys. Rev. B **46**, 6671–6687 (1992).
[18] D. Vanderbilt, Phys Rev. B **41**, 7892–7895 (1990).
[19] H. J. Monkhorst and J. D. Pack, Phys. Rev. B **13**, 5188–5192 (1976).
[20] C. Van de Walle and R. Martin, Phys. Rev. B **34**, 5621–5634 (1986).
[21] J. P. Perdew and M. Levy, Phys. Rev. Lett. **51**, 1884–1887 (1983).
[22] M. C. Toroker, D. K. Kanan, N. Alidoust, L. Y. Isseroff, P. Liao, and E. A. Carter, Phys. Chem. Chem. Phys. **13**, 16644–16654 (2011).
[23] S. Sayan, E. Garfunkel, and S. Suzer, Appl. Phys. Lett. **80**, 2135 (2002).
[24] T. E. Cook Jr., C. C. Fulton, W. J. Mecouch, R. F. Davis, G. Lucovsky, and R. J. Nemanich, J. Appl. Phys. **94**, 7155 (2003).
[25] H. Zhu, G. Ramanath, and R. Ramprasad, J. Appl. Phys. **114**, 114310 (2013).